

Target Specific Hydrogel for Disease Diagnosis and Environmental Remediation

M.Sc. Thesis

By

ANURAG PRIYADARSHI



**DISCIPLINE OF PHYSICS
INDIAN INSTITUTE OF TECHNOLOGY INDORE
JUNE 2022**

Target Specific Hydrogel for Disease Diagnosis and Environmental Remediation

A THESIS

*Submitted in partial fulfillment of the
requirements for the award of the degree
of
Master of Science*

by

ANURAG PRIYADARSHI



**DISCIPLINE OF PHYSICS
INDIAN INSTITUTE OF TECHNOLOGY INDORE**

JUNE 2022



INDIAN INSTITUTE OF TECHNOLOGY INDORE

CANDIDATE'S DECLARATION

I hereby certify that the work which is being presented in the thesis entitled **TARGET SPECIFIC HYDROGEL FOR DISEASE DIAGNOSIS AND ENVIRONMENTAL REMEDIATION** in the partial fulfillment of the requirements for the award of the degree of **MASTER OF SCIENCE** and submitted in the **DISCIPLINE OF PHYSICS, Indian Institute of Technology Indore**, is an authentic record of my own work carried out during the time period from August 2020 to June 2022 under the supervision of Prof. Sudeshna Chattopadhyay, Professor, Discipline of Physics, IIT Indore.

The matter presented in this thesis has not been submitted by me for the award of any other degree of this or any other institute.

Anurag 3/06/2022
**Signature of the student with date
(ANURAG PRIYADARSHI)**

This is to certify that the above statement made by the candidate is correct to the best of my/our knowledge.

Sudeshna
June 3, 2022
Signature of the Supervisor of
M.Sc. thesis (with date)
(Prof. Sudeshna Chattopadhyay)

Anurag Priyadarshi has successfully given his/her M.Sc. Oral Examination held on **6th June 2022**.

Sudeshna
Prof. Sudeshna Chattopadhyay
Signature(s) of Supervisor(s) of MSc thesis
Date: June 6, 2022

Krushna
Signature of PSPC Member
(Prof. Krushna Mavani)
Date: **06/06/2022**

Rajesh
Signature of PSPC Member
(Prof. Rajesh Kumar)
Date: **06/06/2022**

Mandana
Convener, DPGC
Date: **07/06/2022**
Srimanta
Signature of PSPC Member
(Dr. Srimanta Pakhira)
Date: June 06, 2022

ACKNOWLEDGEMENTS

I would like to thank everyone who contributed in some way to the work described in this thesis. First and foremost, I thank my thesis supervisor, Professor Sudeshna Chattopadhyay, for accepting me into her group. During my stint at the Nanomaterials and Energy Research Lab, I have been constantly encouraged by my supervisor to inculcate the scientific thought behind the work I was doing. Her valuable suggestions from time to time have shaped the idea of my work. It has indeed been my pleasure and privilege to have studied a course taught by her.

I would like to thank Dr. Rinki Singh, alumni of IIT Indore, and our lab for giving me an overview of the work I had to proceed with. I am also grateful to my lab members Mr. Vikas, Mr. Arpan, Mr. Ravinder, Mr. Arpan, Mr. Sirsendu and Akash for providing a positive work environment.

I am greatly thankful to Mr. Vikas Munya for his constant support and help throughout my project work. Almost every result described in my thesis was accomplished with his help and support.

Finally, I would thank all my family members for being moral support for me throughout this journey.

Abstract

In the field of healthcare as well as environmental monitoring, the in-situ sensing of chemical parameters such as pH, glucose, enzymes, and other analytes is of immense importance. A considerable number of studies and research work using hydrogel as a chemical/mechanical sensor have been done in this domain. Hydrogels are 3-dimensional networks of cross-linked water-swollen polymers containing chemical groups that are sensitive to environmental stimuli. Hydrogels contain stimuli-sensitive chemical groups, resulting in swelling or shrinking in response to changes in external stimuli. This reversible volume change can be incorporated into magnetic, capacitive, inductive, or other sensing mechanisms. Despite many years of research, hydrogel-based chemo-mechanical sensors have still been beyond practicality. The reasons may have been the difficulties associated with the incorporation of hydrated gel with hard inorganic materials, and the sluggish response of the sensor, among many others. The work presented here is an effort to exhibit a pH-responsive voltage change mechanism of an integrated sensor where the pH response of the pH-sensitive hydrogel is recorded in form of voltage via Arduino sensor, with changes in the distance between the sensor and magnetic strip placed on top of the hydrogel.

TABLE OF CONTENTS

LIST OF FIGURES

LIST OF TABLES

ACRONYMS

Chapter 1: Introduction

1.1 Motivation

1.2 Organization

Chapter 2: Review of Past Work and Problem Formulation

2.1 Introduction to Hydrogels

2.2 Classification of Hydrogels

2.2.1 pH-Sensitive Hydrogels

2.2.2 Thermal-responsive Hydrogels

2.2.3 Electric-responsive Hydrogels

2.2.4 Magnetic-responsive Hydrogels

2.3 Magnetic Materials

Chapter 3: Hydrogel-Magnet Based pH Sensor

3.1 Introduction

3.2 Basic Principle

3.3 Device Design

3.4 Experimental Setup

Chapter 4: Results and Analysis

4.1 Voltage Response Studies

4.2 Swelling Studies

4.2.1 Swelling Reversibility Study

4.3 Discussion

Chapter 5: Conclusion and Scope for Future

REFERENCES

LIST OF FIGURES

Figure No.	Title
Fig. 2.1	Illustration of volume change and swelling ratio curves of anionic and cationic hydrogels in response to pH
Fig. 2.2	Magnetic response of diamagnetic, paramagnetic, ferromagnetic and superparamagnetic materials
Fig. 2.3	Magnetic behavior comparison of ferromagnetic and Superparamagnetic materials in the absence and presence of an external magnetic field
Fig. 3.1	Schematic of the sensing mechanism of the pH sensor, with the magnetic strip height changing in proportion to reversible pH change.
Fig. 3.2	Arduino Uno board
Fig. 3.3 (a)	Hydrogel placed in a vial, kept inside a pH 1.4 solution
Fig. 3.3 (b)	The hydrogel/magnetic strip setup for sensing swelling/shrinking in response to pH change
Fig. 4.1	Voltage response with pH variation between pH 7 and pH 1.4, for Samples 1 and 2
Fig 4.2	Comparison between the voltage outputs for two samples of the same weight.
Fig 4.3	Cycle 1 voltage output from the sensor when hydrogel sample 1 is immersed in pH 7 and in pH 1.4
Fig. 4.4	Cycle 2 voltage output from the sensor when hydrogel sample 1 is immersed in pH 7 and in pH 1.4
Fig. 4.5	Cycle 3 voltage output from the sensor when hydrogel sample 1 is immersed in pH 7 and in pH 1.4
Fig. 4.6	Cycle 1 voltage output from the sensor when hydrogel sample 2 is immersed in pH 7 and in pH 1.4
Fig. 4.7.	Cycle 2 voltage output from the sensor when hydrogel sample 2 is immersed in pH 7 and in pH 1.4
Fig. 4.8.	Cycle 3 voltage output from the sensor when hydrogel sample 2 is

- immersed in pH 7 and in pH 1.4
- Fig. 4.9 (a) pH-dependent three consecutive Swelling (at pH 7) and shrinking (at pH 1.4) behavior of the PAAVSA hydrogel for sample 1.
- Fig. 4.9 (b) pH-dependent three consecutive Swelling (at pH 7) and shrinking (at pH 1.4) behavior of the PAAVSA hydrogel for sample 2.
- Fig. 4.9 (c) Comparison between the swelling/shrinking behaviors of the two samples.
- Fig. 4.10 (a) Sample 1 cycle 1 swelling data when pH of the solution is 7.
- Fig. 4.10 (b) Sample 1 cycle 1 deswelling data for the when pH of the solution changes from 7 to 1.4.
- Fig. 4.11 (a) Sample 1, cycle 2 swelling data when pH of the solution switches from 1.4 to 7.
- Fig. 4.11 (b) Sample 1, cycle 2 deswelling data when pH of the solution switches from 7 to 1.4.
- Fig. 4.12 (a) Sample 1, cycle 3 swelling data when pH of the solution switches from 1.4 to 7.
- Fig. 4.12 (b) Sample 1, cycle 3 deswelling data when pH of the solution switches from 7 to 1.4.
- Fig. 4.13 (a) Sample 2 cycle 1 swelling data when pH of the solution is 7.
- Fig. 4.13 (b) Sample 2 cycle 1 deswelling data for the when pH of the solution changes from 7 to 1.4.
- Fig. 4.14 (a) Sample 2, cycle 2 swelling data when pH of the solution switches from 1.4 to 7.
- Fig. 4.14 (b) Sample 2, cycle 2 deswelling data when pH of the solution switches from 7 to 1.4.
- Fig. 4.15 (a) Sample 2, cycle 3 swelling data when pH of the solution switches from 1.4 to 7.
- Fig. 4.15 (b) Sample 2, cycle 3 deswelling data when pH of the solution switches from 7 to 1.4.

LIST OF TABLES

Table No.	Title
Table 1	Swelling and deswelling characteristics of the PAAVSA hydrogel Sample 1 because of pH reversibility between pH 7 and 1.4
Table 2	Swelling and deswelling characteristics of the PAAVSA hydrogel Sample 2 because of pH reversibility between pH 7 and 1.4
Table 3	Values of swelling rate (SR) and equilibrium swelling (Se) for the PAAVSA hydrogel samples.

ACRONYMS

CGM	Continuous Glucose Monitoring
GERD	Gastroesophageal Reflux Disease
IR	Infrared
LES	Lower Esophagus
MEMS	Micro-Electro-Mechanical Systems
SPIONs	Superparamagnetic Iron Oxide Nanoparticles
PAAVSA	Poly (acrylic acid- <i>co</i> -vinylsulphonic acid)

Chapter 1

Introduction

1.1 Motivation

pH is a key environmental component in the human body, and several diseases, such as gastric reflux disease, cancer, and skin disorders such as dermatitis, ichthyosis, and fungal infection, are characterized by a shift in pH value [1,2,5]. For example, the pH of the tumor site (pH 5), skin tissues in dermatitis (pH 6.6), ichthyosis (pH 4.6 and 5.3), and fungal infections (pH 5.1-5.7), are lesser than pH 7.4, that of normal tissue [7-9].

Diabetes is among the most common medical ailments in the world, which, according to WHO, has affected over 400 million people globally, majorly the people living in lower- and middle-income countries. Diabetes has also directly caused 1.5 million deaths per year. There has been a significant increase in the number of cases and fatalities over the past few decades [13-15].

Its prevalence is estimated to gradually increase in the coming decades due to aging, urbanization, adoption of a sedentary lifestyle, and obesity. By 2030, India's diabetic population is projected to cross 80 million. It suggests that immediate health policy reorganization and investment will be required to make the greatest use of limited healthcare resources and associated economic restrictions. In addition to posing many health concerns for patients and their families, diabetes management also creates a significant financial burden.

According to a recent study, patients in India spend an average of Rs. 10,000 in urban areas and Rs. 6260 in rural regions on diabetes care per year. According to diabetic studies, the direct and indirect costs of diabetes are multifold all over the world [16,17].

A low-cost, accurate, and continuous glucose monitoring system can significantly reduce diabetes management costs by allowing the patients to have tighter control over their blood glucose levels. Diabetes refers to two types of malfunctions in glucose homeostasis. Diabetics suffering from Type I exhibit wide swings in blood glucose due to the destruction of pancreatic beta cells, which secrete and regulate insulin, by a cell-specific autoimmune process [10,18]. A scarcity of these cells causes an elevated blood glucose level (hyperglycemia), which can result in blindness or deterioration of muscle, nerve, and connective tissue. Type I diabetes can be treated by insulin injection via either a syringe or a wearable pump. Regardless of the method used, precise and accurate dosing is of utmost importance. An underdose of insulin would lead to undertreatment, and an overdose could result in a subnormal blood glucose level (hypoglycemia), leading to a subnormal blood glucose level (hypoglycemia) disorientation, coma, or death. To maintain stable and adequate blood glucose levels using discrete dosing, it is important to frequently monitor the blood glucose level. Type II is characterized by suboptimal utilization of secreted insulin for managing blood glucose levels. This is typically a result of increased consumption of unhealthy food as well as a sedentary lifestyle. The first line of treatment for type II diabetes is pharmaceutical and lifestyle modifications (more physical activity and weight reduction). Nevertheless, monitoring glucose levels remains a core part of the treatment [11].

Diabetic patients usually monitor their blood glucose level intermittently via the finger-stick method. However, this technique is inconvenient and uncomfortable, especially for children, the elderly, bed-ridden, or handicapped patients. In addition, since this provides only discrete observations of blood glucose level, which changes continuously with time, important fluctuations in the level might be missed. To address this issue, there have been substantial developments in Continuous Glucose Monitoring systems (CGMs) the enhanced diabetic care and treatment [19-21]. CGMs can measure blood glucose levels in real-time and record, save, and communicate the information wirelessly.

Current commercial CGM systems feature percutaneous glucose electrodes, with a working mechanism that relies on the oxidation of glucose [22-25]. There are various practical concerns including the need for periodic calibration of CGMs against blood glucose levels acquired by the finger-stick method and the risk of infection from the dermal breach. Thus, there has been a growing interest in developing long-term and implantable CGMs [26-28]. Several CGM systems have been demonstrated using diverse methods including absorption and reflectance of near- and far-IR radiation [29-30], surface-enhanced Raman scattering [31], and fiber optics with glucose-sensitive phenylboronic acid-based hydrogels [32,33]. These approaches confirmed the glucose-sensing principles, but their practical utility has been hindered by their unreliability when used in vivo, and inconvenient readout systems. Hence, a simple, cost-effective, continuous, wireless, and easy-to-use monitoring system is the need of time.

Gastroesophageal reflux disease (GERD) is another widely found medical condition across the globe. It is estimated to increase gradually due to fast-moving lifestyles and bad food habits [2]. The food we swallow goes down the esophagus and passes through the lower esophageal sphincter (LES). Normally, the LES opens to get food into our stomach and then closes to prevent the food and acidic stomach juices flow back into our esophagus. But when LES gets weaker, the stomach contents flow up into the esophagus, causing gastroesophageal reflux. The most common symptoms are burning sensations in the chest (heartburn), regurgitation, and an acidic taste in the back of the mouth. Heartburn typically occurs after eating and may worsen at night [34].

Presently, GERD is diagnosed by an esophageal pH test. It is an outpatient procedure performed to measure the pH or amount of acid that flows into the esophagus from the stomach within 24 hours [4].

The equipment used in the gastroesophageal pH test consists of a small probe that is inserted through the patient's nostril and positioned near the lower esophagus. The probe is plugged into a recorder worn on a belt

or over the waistband [35-37]. A newer, wireless device may make monitoring the pH level easier: Instead of having to have a tube placed down to the patient's nose for 24 hours, a disposable capsule is placed into the esophagus using an endoscope. The capsule then wirelessly transmits information for up to 48 hours to a receiver (about the size of a pager) worn around the waist. The receiver has several buttons on it that should be pressed to record symptoms of GERD such as heartburn, chest pain, regurgitation, etc. A diary is maintained to keep track of events like sleeping, eating, drinking, lying down, and getting up. Though this method of pH monitoring is effective, it is kind of annoying also. Every time one must press the button on the recorder when a symptom arises, even if it is minor. The capsule measures pH levels in the esophagus and transmits readings to the receiver. Real-time and continuous monitoring is a dire need to make the GERD treatment more effective without disturbing the patients' sleep routine and consciousness.

Hydrogels, one of several alternative sensing materials, have been extensively investigated for use in pH and glucose monitoring systems for a variety of reasons, owing to their wide range of features. To begin with, hydrogels, which are water-swollen polymer networks, contain chemical groups that are responsive to environmental stimuli including pH, temperature, and glucose. When the polymers are physically triggered (for example, by a change in temperature), they show additional and reversible volumetric behavior, such as shrinking or swelling. A chemical interaction (e.g., pH or glucose) between an analyte of interest and a moiety contained within the hydrogel can also cause a volume response. In either scenario, the chemo-mechanical swelling and shrinking of hydrogels in response to stimuli can be used as a signal transduction process, eliminating the need for an electrical power supply. The high water content of hydrogels provides a dependable aqueous interface for greater transport of environmental analytes into the hydrogel matrix, which is the second reason for their use. The ease with which hydrogels can be bio/chemically

functionalized with molecules and other nano-scale entities during the crosslinking process is the third advantage [38,39]. Magnetically guided medication delivery to the site of interest, for example, can be achieved using superparamagnetic nanoparticles embedded in a pH-sensitive hydrogel. This specific functionalization capability enables the use of hydrogel for a variety of stimuli sensing applications, including glucose, pH, temperature, and so on. Despite these benefits, hydrogel-based monitoring devices are not currently in use in clinical settings. This is because soft hydrogels are difficult to handle and localize in tough environments like the human body. Due to the diffusion-limited response of hydrogels to stimuli, the reaction time quadratically rises with size [40]. Finally, sophisticated readout systems are necessary when hydrogel-based sensors are implanted in the human body to monitor their chemo-mechanical activity. To solve these difficulties, more stiff, easier-to-handle substrates must be integrated with hydrogel devices to build more medically practical systems. This project aims to create a simple and easy to fabricate hydrogel-based system.

1.2 Organization

This thesis consists of five chapters. Chapter 1 briefly addressed the motivation and significance of the proposed research. Chapter 2 focuses on understanding background knowledge for the ultimate goal of this master's work. In the beginning, the classification of hydrogels is described followed by the chemical behavior of four kinds of hydrogels, namely, pH-responsive, thermal-responsive, electric- and magnetic-responsive hydrogels. Afterward, the fundamental physics of magnetic materials for understanding superparamagnetic hydrogels is described. In the following chapter 3, a hydrogel-magnet-based remote pH interrogation scheme was demonstrated. As the hydrogel responds to the pH change, the varied magnetic field is sensed by Arduino sensor which indicates the swelling/shrinking of the hydrogel, or indirectly the pH of the solution. Chapter 4 covers the results and analysis of the sensing

scheme discussed in chapter 3. Chapter 5 draws the conclusion from the results and discusses on prospective research for the improvement of the hydrogel-based chemical sensing devices.

Chapter 2

Background on: Hydrogels and Magnetic Materials

2.1. Introduction to Hydrogels

Hydrogels are a three-dimensionally crosslinked polymer networks exhibiting a swelling capacity when immersed in aqueous media such as water [41]. The hydrophilicity of functional groups integrate into in backbone chains of hydrogels allows them to uptake a large amount of water up to several times their weight and isotropically expand while preserving their shape and structure [42]. The degree of volume enlargement depends on the count of water contained in the hydrogel and shows reversibility; hydrogels swell in the presence of water and shrink in its absence.

2.2. Classification of Hydrogels

Hydrogels can be generally classified into two groups based on the type of crosslinking: physically crosslinked and chemically crosslinked hydrogels [43].

In reversible (or physical) hydrogels, polymeric networks are held together by molecular entanglements or secondary forces including ionic, hydrogen bonding, or hydrophobic interactions. Reversible interactions can be disrupted by changes in physical conditions or stress.

Permanent (or chemical) hydrogels have covalently crosslinked networks, hence they are stronger and more stable than physically bonded hydrogels. Their equilibrium swelling state depends on the polymer-water interaction parameter and crosslink density.

For both gels, chemically or physically crosslinked polymer chains prevent hydrogels from dissolution. The ability of hydrogels to custom construct their chemical composition, allowing them to respond to physiological conditions, is a remarkable feature that has sparked a lot of attention (e.g. pH, glucose, etc.). Hydrogels have additional swelling and deswelling as a result of changes in stimuli (e.g., pH changes from acidic to basic). The volumetric response changes dramatically due to functionally sensitive chemical groups integrated in their backbone chains, which are also reversible [44]. Hydrogels vary their size and shape as well as their mechanical strength and permeability when they interact with physical (e.g. temperature) or chemical (e.g. pH and glucose concentration) stimuli. Hydrogels have been widely used in a variety of applications, including biosensors, drug delivery devices, chemical valves, and bioseparation, due to the aforementioned features [45,46].

Among the above applications, the primary focus was to develop a passive chemical sensing method utilizing the smart characteristics of hydrogels, particularly for pH monitoring. In the work presented, one such hydrogel-based monitoring system was studied.

2.2.1. pH-sensitive hydrogels

pH-sensitive hydrogels with ionic functional groups vary their volume behaviour abruptly or gradually in response to changes in the surrounding environment's pH levels. Anionic (e.g. carboxyl acid, sulfonic acid) or cationic pendant groups can be found in hydrogels (e.g. amines). Different kinetics of swelling and shrinking exist depending on the side groups of the polymer networks. When the pH of a media is higher than the pKa of the pendant groups, anionic hydrogels swell due to the ionisation of the pendant groups.

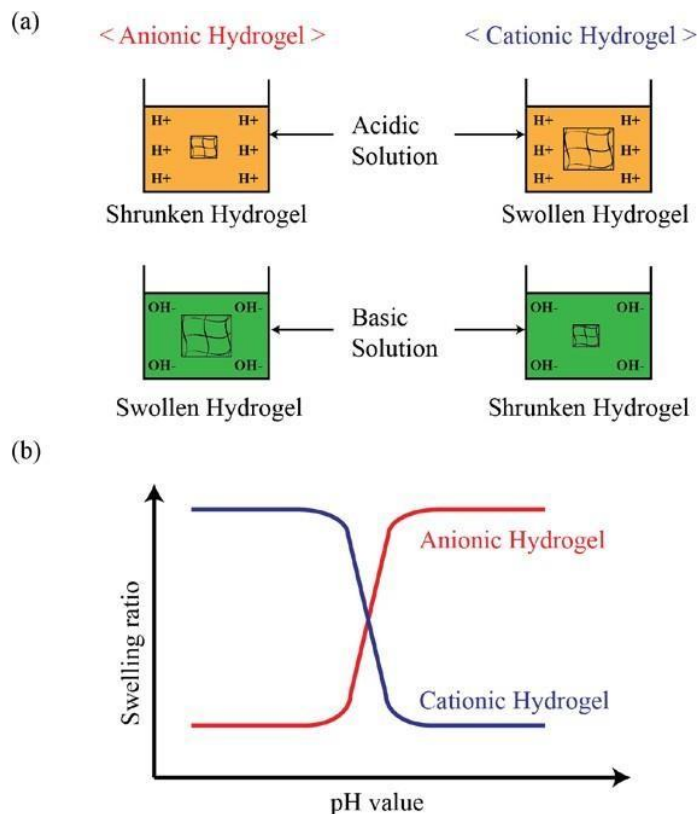


Fig. 2.1. Illustration of (a) volume change and (b) swelling ratio curves of anionic and cationic hydrogels in response to pH [44].

The increased electrostatic repulsion force between the groups is caused by the high degree of ionisation. As a result, the polymer's hydrophilicity rises, resulting in a higher swelling reaction. Cationic hydrogels, on the other hand, ionise at a pH lower than the groups' pKa. When exposed to a low pH environment, they swell due to enhanced hydrophilicity as a result of the higher repulsion force. At either low or high pH values, the protonation of the ionised side groups causes the hydrogels to shrink, resulting in a lower repulsion force. The volume responses and swelling ratio curves of anionic and cationic hydrogels in acidic and basic solutions are depicted in Figure 2.1. The swelling ratio is calculated by dividing the swollen weight by the dried weight.

2.2.2. Thermal-responsive hydrogels

These are temperature-sensitive hydrogels. When there is a temperature change, these hydrogels start releasing drugs or moisture, which is reversible upon cooling. These hydrogels contain both hydrophobic and hydrophilic components in structures generally, and the phenomenon of thermal response is derived from the delicate balance between the hydrophobic and hydrophilic portions of the polymer monomer. temperature changes the interaction between hydrophilic and hydrophobic segments in the polymer with water molecules and thus can induce a change in the solubility of the cross-linked network. For example, Poly(N-isopropyl acrylamide).

2.2.3. Electric-responsive hydrogels

Electric-responsive hydrogels, when exposed to an electric field, change their geometrical shapes and sizes by swelling/shrinking. The electric-responsive behavior of these hydrogels is often realized in an electrolyte aqueous environment, and the directional migration of mobile ions (i.e., cations to a cathode and anions to an anode) in the hydrogel–electrolyte solution system occurs under the applied electric stimuli[48].

2.2.4. Magnetic-responsive hydrogels

These are modified normal hydrogels with magnetic-responsive nanoparticles. With the integration of these magnetic materials, the inherently nonmagnetic-responsive hydrogels become sensitive to external magnetic stimuli, hence demonstrating magnetically actuated deformation and movement [49].

2.3. Magnetic Materials

Magnetic materials are used in biomedical devices and equipment for MRI, cell separation, targeted medication, gene delivery, and

hyperthermia [49]. In recent years, nanoscale magnetic materials have piqued curiosity. This is owing to the capacity to synthesis nanoparticles with size-controlled between a few nanometres and a few tens of nanometres. Furthermore, biological molecules can be used to functionalize nanoparticles in order to trap, segregate, and detect viruses, DNA, and proteins [50]. Magnetic materials can be influenced by an external direct or alternating magnetic field. This characteristic can be used for cell separation, drug targeting, and hyperthermia, among other things. Nano-scale compounds can also be suspended in an aqueous solution or immersed in a solid (e.g. polystyrene) or viscous (e.g. hydrogel) substance to change their magnetic properties, depending on the application.

When an external magnetic field is applied to magnetic material they respond differently depending on the nature and atomic structure of the material. The magnetic induction due to an external field can be expressed by: $B = \mu_0(H+M)$.

where μ_0 is the permeability of free space, H is the external magnetic field strength, B is the magnetic induction in the material, and M is magnetization. The magnetization M, which is the magnetic moment (m) per unit volume of the material, is related to the field strength H and volumetric magnetic susceptibility χ by: $M = \chi H$.

Susceptibility is dimensionless in SI units, although M and H are both in Am⁻¹. Magnetization is a significant determinant of magnetic induction with a given magnetic field intensity, as can be seen from the equations above. Susceptibility, or the degree of magnetization in response to an imposed field, varies based on the type of magnetic material. In general, diamagnetic, paramagnetic, ferromagnetic, and superparamagnetic substances are divided into four categories [51]. For each type of material, Figure 2.2 demonstrates the relationship between magnetic field strength and magnetization. Atoms in diamagnetic materials have paired electrons that spin in opposite directions. As a result, there are no net magnetic dipole moments in the substances.

When the materials are subjected to an external magnetic field, the orbital motion of the electrons asymmetrically alters, resulting in a very modest net magnetization that points in the opposite direction of the field. (Fig. 2.2 (a)). The susceptibility of diamagnetic materials normally falls in the range of -10^{-6} to -10^{-3} . In comparison with diamagnetic materials, atoms of a paramagnetic particle possess unpaired electrons with no pair of spins in the opposite directions; hence, individual atoms exhibit inherent magnetic dipole moments without an external magnetic field. However, no magnetization is observed when viewed as a collection of atoms in paramagnetic materials because the magnetic dipole moments of each atom are randomly oriented, and they are canceled by each other. When located at a magnetic field, however, the dipole moments are inclined to align along the field showing a large magnetization with the parallel direction of the field (Fig. 2.2 (b)). The susceptibility of paramagnetic materials is typically in the range from 10^{-6} to 10^{-1} . For both diamagnetic and paramagnetic materials, the magnitude of their magnetization is proportional to the imposed magnetic field.

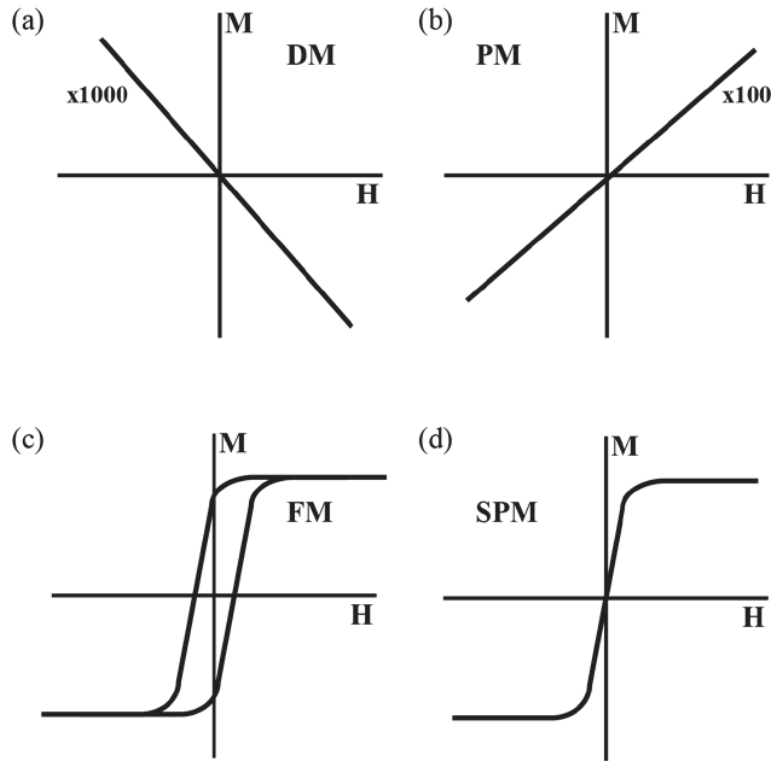


Fig. 2.2. Magnetic response of magnetic materials ((a) DM: diamagnetic, (b) PM: paramagnetic, (c) FM: ferromagnetic, (d) SPM: superparamagnetic) [51].

When the atoms come closer to each other, their magnetic dipole moments spontaneously communicate with adjacent dipole moments resulting in long-range order of the orientation of the dipole moments. As a result of this event, a magnetic domain with a favored orientation forms. Because of their random orientations, ferromagnetic substances, which are made up of several such domains, have no magnetism. However, when a magnetic field is applied, the materials are easily magnetized because their domains prefer to align with the field's analogous direction. Unlike diamagnetic and paramagnetic materials, ferromagnetic materials with a relatively high susceptibility have hysteresis in the M-H curve (Fig. 2.2 (c)). The magnetic domain walls are eliminated when the imposed field is sufficiently high, and saturation magnetization occurs [52]. When the field is removed, remanent

magnetization remains because the replicated domain walls are more likely to settle at energy minima rather than revert to their original places. To disorient the magnetic dipole moments of the domains, external energy is necessary. For example, heating the substance to a temperature over the curie temperature can cause the remanent dipole moments to relax. As previously stated, the hysteresis of ferromagnetic materials is attributed to arbitrarily oriented magnetic multiple domains, each of which is made up of aligned moments to the domain's easy axis. However, by reducing the size of materials below a certain value based on the material type, the dimension of hysteresis can be lowered. Materials with a diameter of tens of nanometres or less eventually retain a single magnetic domain. When subjected to an external magnetic field, these materials behave similarly to multi-domain materials. Magnetic dipole moments, on the other hand, relax fast when the applied field is withdrawn due to thermal energy. As a result, as illustrated in Figure 2.2, it causes the removal of net magnetization with no hysteresis (d). This is referred to as superparamagnetism.

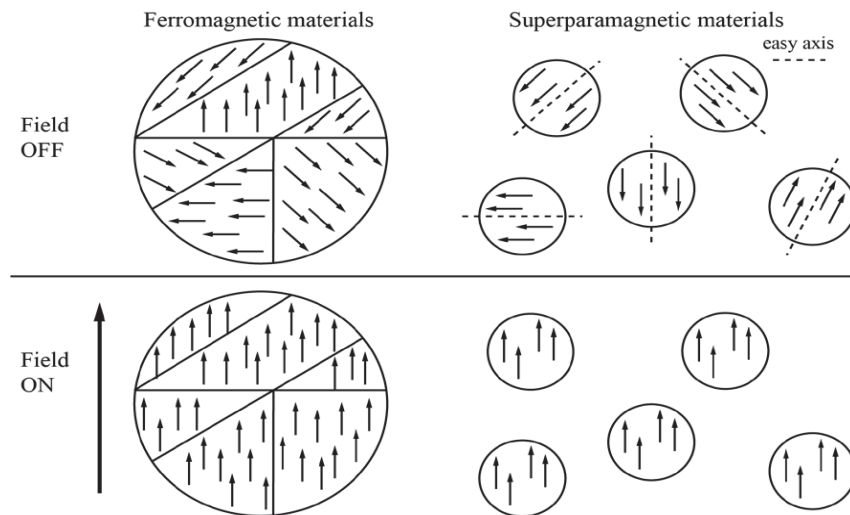


Fig. 2.3. Magnetic behavior comparison of ferromagnetic and superparamagnetic materials in the absence (top) and presence (bottom) of an external magnetic field [53].

The magnetic behaviour of ferromagnetic and superparamagnetic materials in the absence and presence of a magnetic field is depicted in Figure 2.3. Furthermore, superparamagnetic materials act in the same way as paramagnetic materials, but they execute a stronger alignment of magnetic dipole moments, resulting in higher susceptibility and saturation magnetization.

In the absence of a magnetic field, superparamagnetic substances have thermal energy-induced flipping of net magnetic dipole moments, resulting in no remaining magnetization.

Chapter 3

Hydrogel-Magnet based pH Sensor: Design and Experimental Setup

3.1 Introduction

With the advancements in sensor designing, we have the availability of very sophisticated MEMS-based chemical sensors. They are although very good at working, their design and fabrication are very complicated and at the microlevel, requiring photolithography technique for preparing the components and the same sophisticated circuitry. Therefore, a potential solution to the aforementioned hitch is simply to place a light magnetic strip on top of a hydrogel film. The swelling and shrinking responses of the hydrogel to chemical stimuli such as pH and glucose concentrations result in vertical movement of the magnet strip, and the amount of swelling/shrinking can be monitored by an Arduino sensor. Since Arduino sensors can detect small changes in a magnetic field, they are uniquely suited for this application. In the following sections, the design, operating principle, and experimental results will be discussed.

3.2 Basic Principle

The PAAVSA hydrogel shows anionic behavior due to the constituent anionic functional groups acrylic and vinylsulphonic acid. When this hydrogel is immersed in pH 7 solution, the ionization of these groups in the PAAVSA hydrogel increases [54], causing a large electrostatic repulsion between nearby ionized COO^- and SO_3^- groups of the network

structure, and the concentration of ions inside the hydrogel increases than in the surrounding solution, creating an osmotic pressure difference between the two and thereby resulting in the expansion and change in the dielectric of the hydrogel network [57,58]. Now, as the hydrogel swells, the magnetic strip placed on the top of it gets closer to the Arduino sensor, making more magnetic field lines from the magnetic strip pass through the sensor and giving higher voltage output through it.

When the PAAVSA hydrogel is dipped in pH 1.4 solution, an increase in H^+ ion concentration causes recombination of H^+ ions with the constituent functional groups and results in the shrinking of the network. As the hydrogel shrinks, the magnetic strip placed on top of the hydrogel goes farther from the Arduino sensor letting a lesser number of magnetic field lines from the magnetic strip pass through the sensor, thereby giving weaker voltage output through it.

The Arduino sensor senses the magnetic field. Arduino board comprises six ADC channels, as shown in Fig. 3.1. Among those, any one or all of them can be used as inputs for analog voltage. The Arduino Uno ADC is of 10-bit resolution. This means that it will map input voltages between 0 and 5 volts into integer values between 0 and 2^{10} . Therefore, the ADC resolution is $5000 \text{ mV}/1024 = 4.88 \text{ mV}$. When there is any change in the magnetic field surrounding the Arduino sensor, an ADC value is reflected on the screen connected to the pins on the Arduino board. That ADC value is converted to a discrete analog voltage by multiplying the ADC value into ADC resolution, 4.88 mV.



Fig. 3.1. Arduino Uno board.

3.3. Device Design

A cross-sectional schematic of the hydrogel/ magnet pH sensor and its operation principle is described in Figure 3.2. The sensor consists of a light polymeric magnet placed on top of a hydrogel surface, which, in response to any variation in the external environment i.e. pH, vertically moves up (showing swelling) and down (showing shrinking). This vertical movement of hydrogel is periodically monitored by an external Arduino sensor fixed at a proper distance from the hydrogel-magnetic strip bilayer.

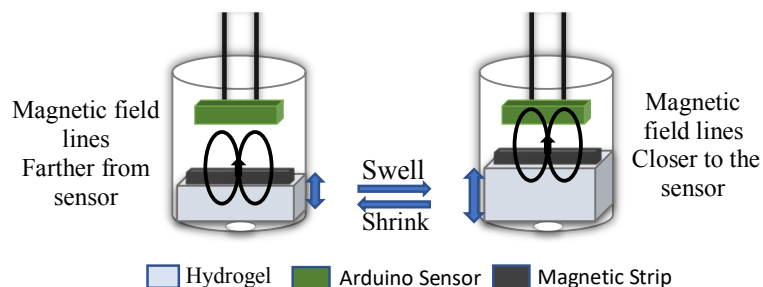


Fig. 3.2. Schematic of the sensing mechanism of the pH sensor, with the magnetic strip height changing in proportion to reversible pH change [59].

3.4. Experimental setup

The pH-responsive pre-synthesized poly (acrylic acid-co-vinylsulphonic acid) hydrogel (PAAVSA) was used to create the hydrogel-magnet bilayer sensor to provide a working prototype [54]. To make the device, first, a sample of 84 mg dry PAAVSA hydrogel was taken. Next, a vial was taken, and a small hole was made on its bottom layer to let the pH solution from a beaker cross through into the vial and immerse the hydrogel sample kept inside it. The hydrogel sample, which was inside the vial, was placed in the beakers having 100 ml buffer solutions of different pH (7 and 1.4, respectively) at room temperature. The monomers of PAAVSA hydrogel being anionic, exhibit higher swelling when the pH of the solution is 7. The vertical swelling behavior was monitored at regular intervals via Arduino sensor by every time taking the vial out of the beaker and placing a magnetic strip on top of the hydrogel, inside the vial.

The procedure was continued until the hydrogel attained a constant weight. This was confirmed by measuring the weight of the hydrogel as well as from the ADC values obtained via the Arduino sensor.

Further, a similar procedure was repeated with the pH of the solution changed to pH 1.4. Thereafter, the hydrogel exhibited shrinking, and the swelling ratios and voltage values also showed a decrease with time.

This swelling/shrinking of the hydrogel was studied in three cycles for two different samples of the same weights to show reversibility and draw a comparison and extract the relation between the pH variation and voltage change as measured via the Arduino sensor.

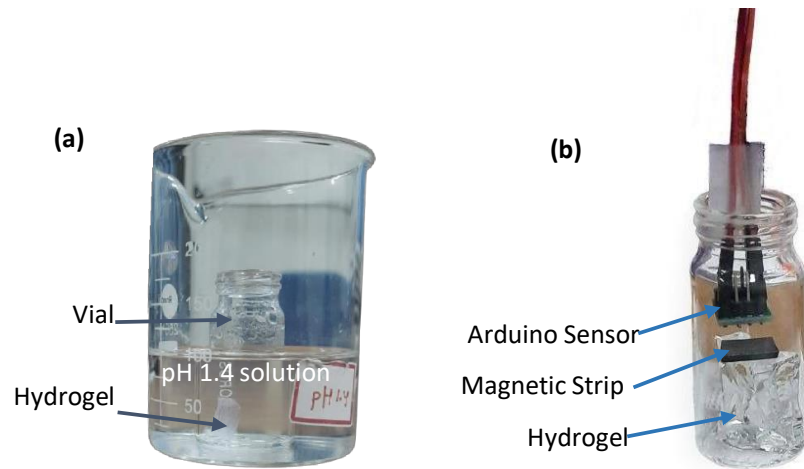


Fig. 3.3. (a) Hydrogel placed in a vial, kept inside a pH 1.4 solution; (b) The hydrogel/magnetic strip setup for sensing swelling/shrinking in response to pH change.

Chapter 4

Results and Analysis

4.1. Voltage response studies

As mentioned in the earlier section, the voltage response study through the Arduino sensor was studied at regular time intervals. This study was parallelly performed with the swelling study [54].

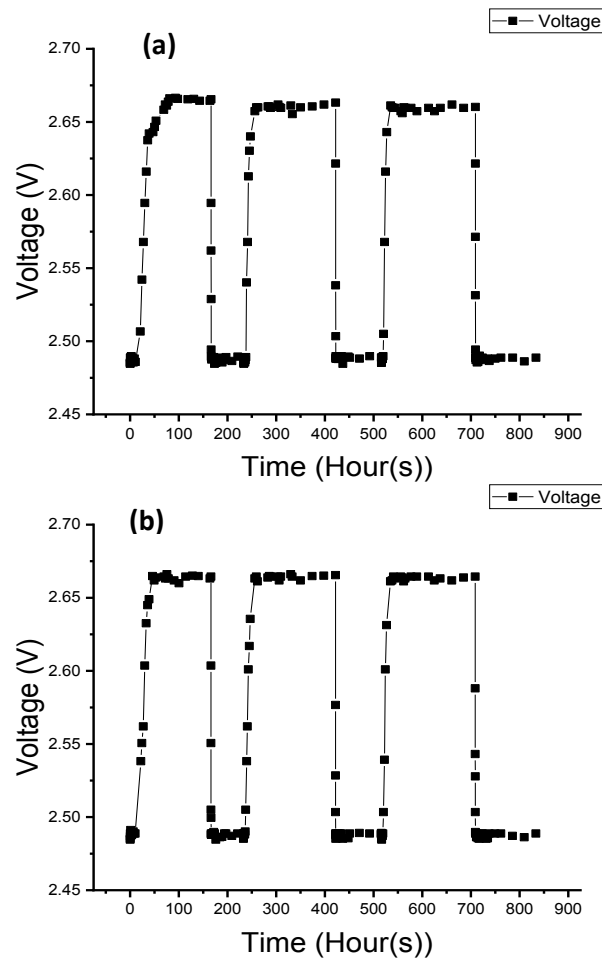


Fig 4.1. Voltage response with pH variation between pH 7 and pH 1.4, for (a) Sample 1; and (b) Sample 2.

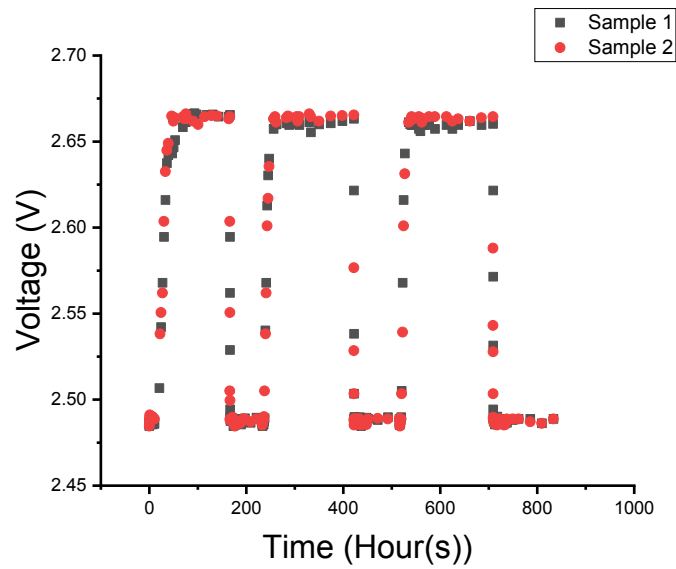


Fig 4.2. Comparison between the voltage outputs for two samples of the same weight.

Figures 4.1 and 4.2 showed that data of voltage response when the hydrogel samples weighting 84 mg were initially placed at an optimized 3.1 cm distance from the Arduino sensor. The figures draw a comparison between the voltage outputs taken in regular time intervals for the two hydrogel samples, showing almost similar response which is analyzed further in details.

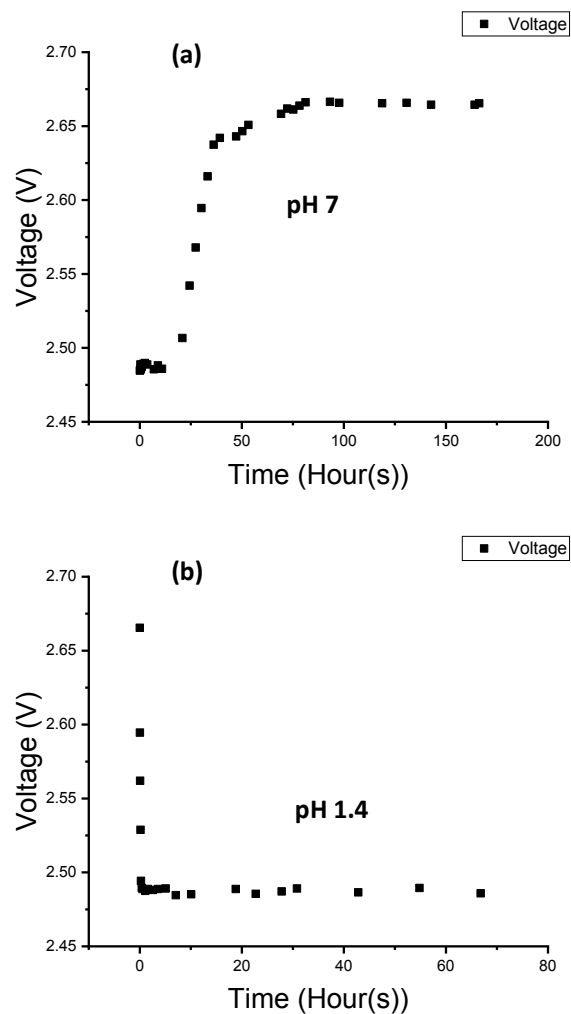


Fig 4.3. Cycle 1 voltage output from the sensor when hydrogel sample 1 is immersed in (a) pH 7; and in (b) pH 1.4.

Fig 4.3 (a) showed that when hydrogel was periodically dipped in pH 7 solution, the Arduino sensor started sensing an increase in the magnetic field from 20.9 hours, increasing until 72 hours when it achieves maximum output. The rate of voltage increase was 0.013 V/hr.; (b) showed a swift decrease in the voltage output which reached its minimum value after 14 minutes since the hydrogel was dipped in pH 1.4 solution. The rate of decrease was 1.552 V/hr.

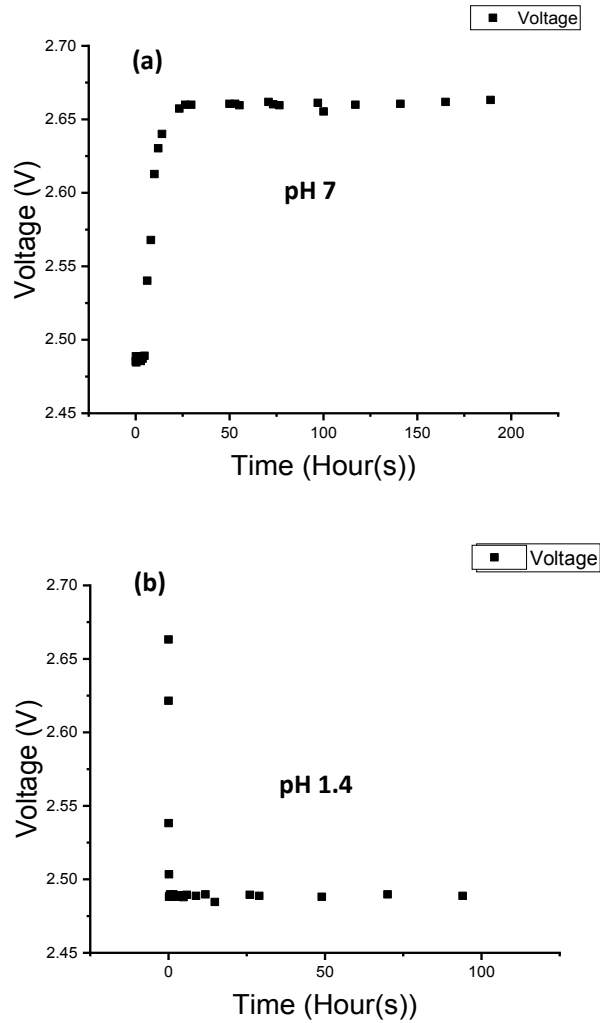


Fig. 4.4. Cycle 2 voltage output from the sensor when hydrogel sample 1 is immersed in (a) pH 7; and in (b) pH 1.4.

Fig 4.4 (a) showed that when hydrogel was periodically dipped in pH 7 solution, the Arduino sensor started sensing an increase in the magnetic field after 4.67 hours, increasing until 29.53 hours when it attained nearly maximum output. The rate of increase was 0.0242 V/hr.; (b) showed a swift decrease in the voltage output which reached its minimum value after 14 minutes since the hydrogel was dipped in pH 1.4 solution. The rate of decrease was 1.56 V/hr.

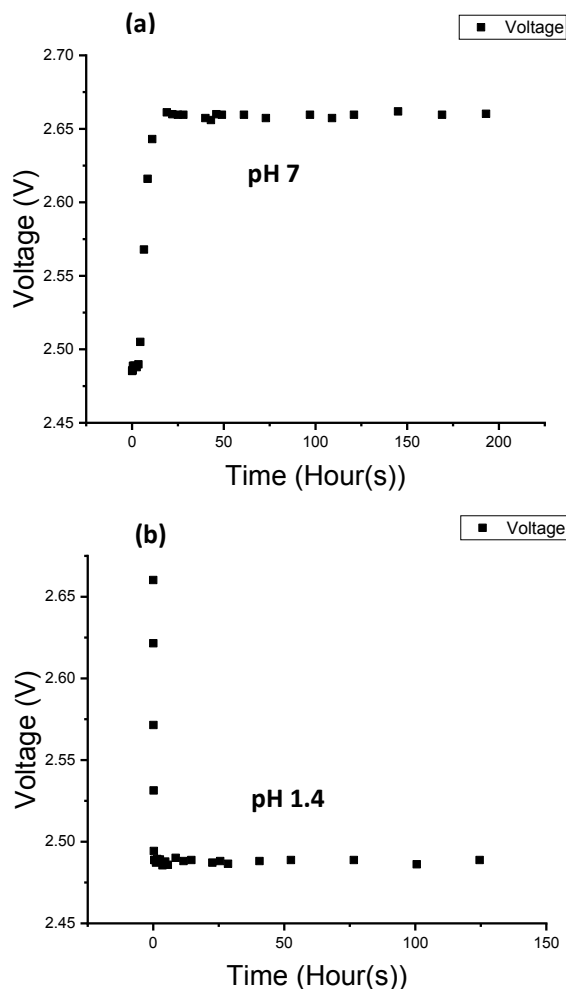


Fig. 4.5. Cycle 3 voltage output from the sensor when hydrogel sample 1 is immersed in (a) pH 7; and in (b) pH 1.4

Fig 4.5 (a) showed that when hydrogel was periodically dipped in pH 7 solution, the Arduino sensor started sensing an increase in the magnetic field after 4.5 hours, increasing until 19 hours when it attained nearly maximum output. The rate of increase was 0.033 V/hr.; (b) showed a swift decrease in the voltage output which reached its minimum value after 14 minutes since the hydrogel was dipped in pH 1.4 solution. The rate of decrease was 1.56 V/hr.

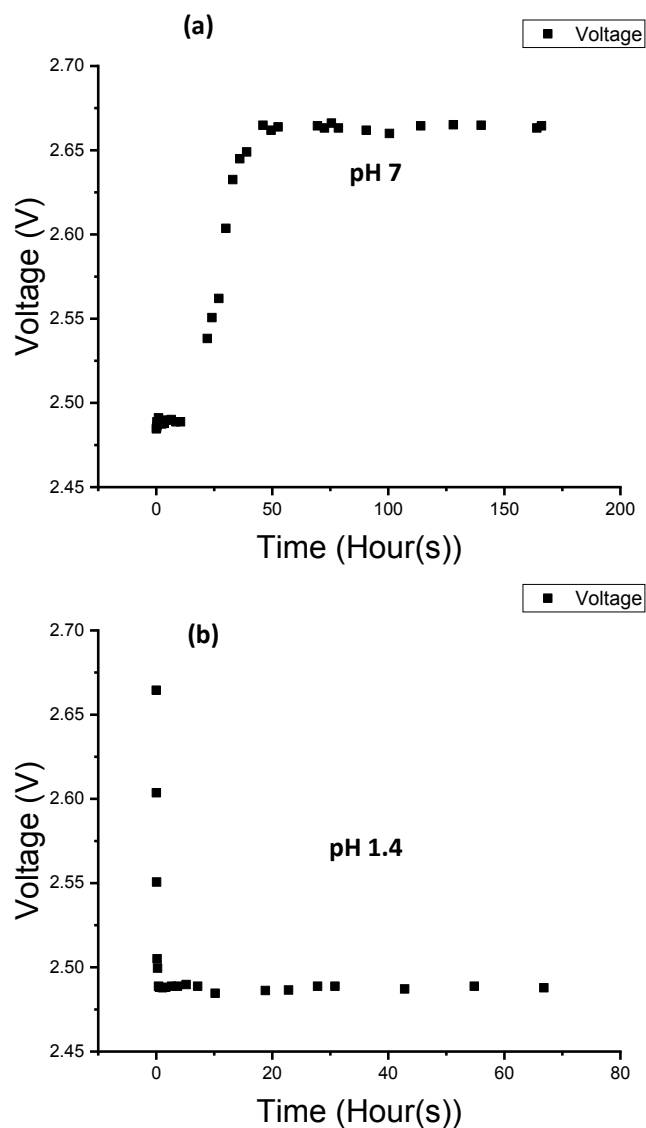


Fig. 4.6. Cycle 1 voltage output from the sensor when hydrogel sample 2 is immersed in (a) pH 7; and in (b) pH 1.4

Fig 4.6 (a) showed that when hydrogel was periodically dipped in pH 7 solution, the Arduino sensor started sensing an increase in the magnetic field from 22 hours, increasing until 46 hours when it got nearly maximum output. The rate of increase was 0.027 V/hr.; (b) showed a swift decrease in the voltage output which reached its minimum value after 14 minutes since the hydrogel was dipped in pH 1.4 solution. The rate of decrease was 1.547 V/hr.

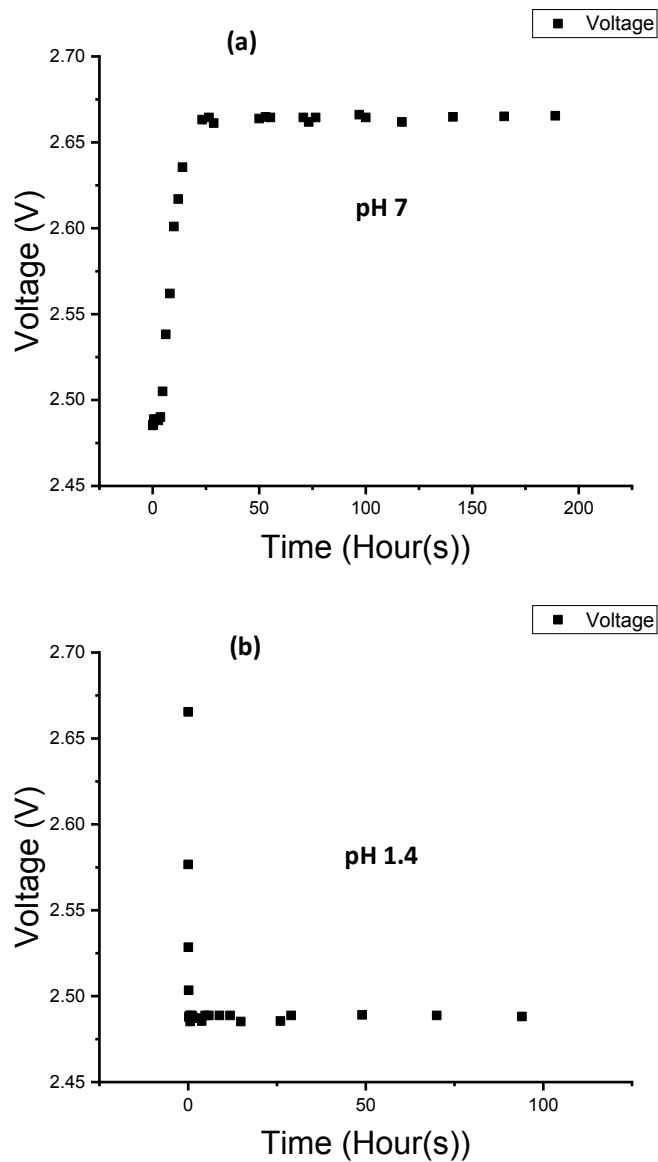


Fig. 4.7. Cycle 2 voltage output from the sensor when hydrogel sample 2 is immersed in **(a)** pH 7; and in **(b)** pH 1.4

Fig 4.7 (a) showed that when hydrogel was periodically dipped in pH 7 solution, the Arduino sensor started sensing an increase in the magnetic field from 4.67 hours, increasing until 28.67 hours when it attained nearly maximum output. The rate of increase was 0.021 V/hr.; (b) showed a swift decrease in the voltage output which reached its minimum value after 14 minutes since the hydrogel was dipped in pH 1.4 solution. The rate of decrease was 1.587 V/hr.

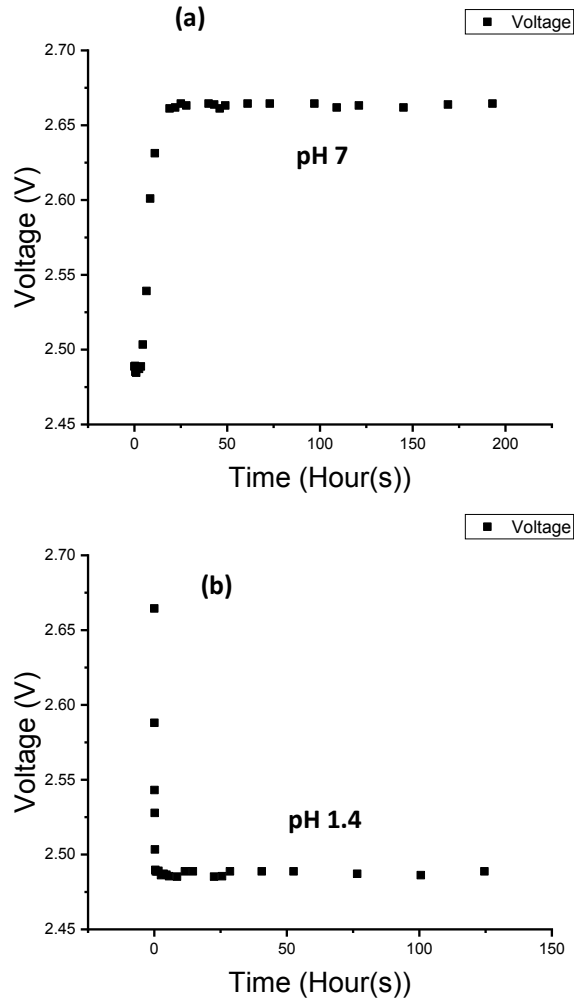


Fig. 4.8. Cycle 3 voltage output from the sensor when hydrogel sample 2 is immersed in **(a)** pH 7; and in **(b)** pH 1.4

Fig 4.8 (a) showed that when hydrogel was periodically dipped in pH 7 solution, the Arduino sensor started sensing an increase in the magnetic field after 4.5 hours, increasing until 19 hours when it attained nearly maximum output. The rate of increase was 0.027 V/hr.; (b) showed a swift decrease in the voltage output which reached its minimum value after 14 minutes since the hydrogel was immersed in pH 1.4 solution. The rate of decrease was 1.587 V/hr.

The voltage response study from two samples of the same hydrogel amount and shape revealed that in cycle 1, a longer time was taken for the sensor to see an increase in the voltage output, as compared to cycles 2 and 3, for pH 7. The reason behind this was that initially, hydrogel was in a dry state and the vertical separation between the magnetic strip placed on top of hydrogel and the sensor was farther, taking a longer time to gain weight and get closer to the sensor. Whereas in the second and third cycles for pH 7, the hydrogel had already gained some extra weight before a transition from pH 1.4 to 7.

The findings reveal very high sensitivity to the observed pH values in form of changes in voltage output as read via the Arduino sensor, showing an increasing rate of around 0.25 V/hr when hydrogel is kept in pH 7 solution, whereas a decreasing rate of around 1.56 V/hr when the hydrogel is kept in pH 1.4 solution. The much higher sensitivity in the given pH range makes our experimental setup a promising tool for sensing diseases where pH abruptly falls and rises.

4.2. Swelling studies

The pH-responsive swelling behaviour of PAAVSA hydrogel was studied and is presented in the figures 4.9 and 4.10. The swelling properties of the two hydrogel samples having the same shape and size were investigated by calculating their swelling ratios. In a typical procedure, a weighted 84 mg of dry hydrogel sample was dipped alternatively in 100 ml of solutions having pH values of 7 and 1.4, respectively at room temperature. As the hydrogel exhibited swelling and shrinking in pH 7 and 1.4 solutions, respectively, the solution pH was bound to change slightly which was maintained from time to time by adding some volume of 0.5M HCl and 0.5 M NaOH, accordingly. During the swelling study, the wet hydrogel was taken out from pH solutions in regular intervals to measure the instantaneous weights after filtering excess water from the hydrogel. This process continued till swelling/shrinking equilibrium was achieved. The swelling ratio (Q) was calculated using the following equation [55].

$$Q = \frac{(W_s - W_d)}{W_d} \quad (1)$$

Where, W_s and W_d are the weights of the swollen and dried hydrogels, respectively.

4.2.1 Swelling reversibility study

The pH sensitivity of PAAVSA hydrogel was studied by performing a swelling/shrinking study at room temperature with pH values of 7 and 1.4. Figure 4.9 shows the swelling /shrinking behavior for the two 84 mg of the initial dry hydrogel samples.

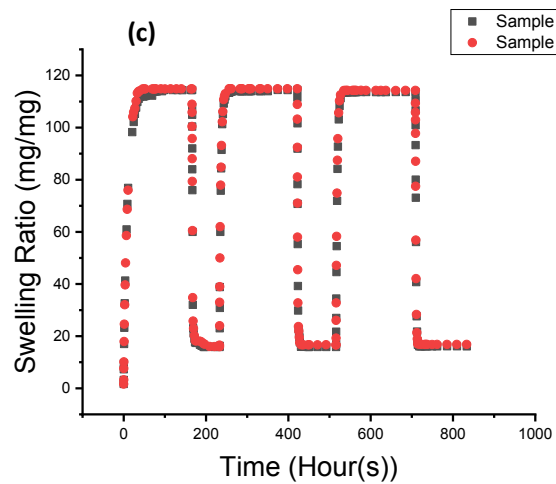
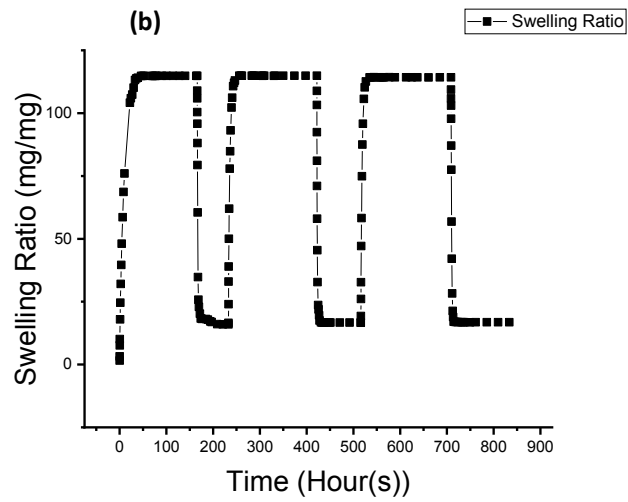
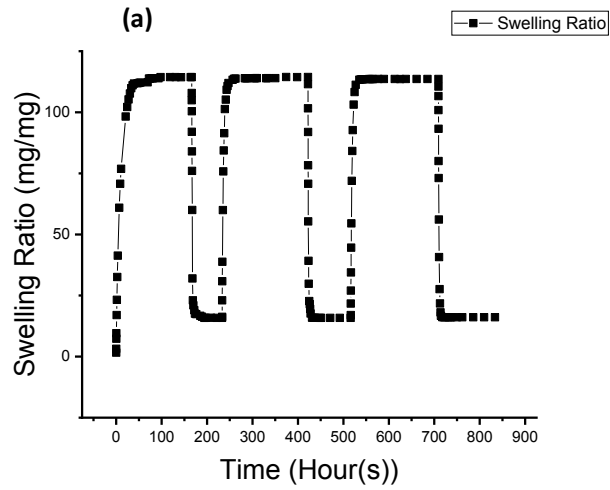


Fig. 4.9. pH dependent three consecutive Swelling (at pH 7) and shrinking (at pH 1.4) behavior of the PAAVSA hydrogel: **(a)** for sample 1; **(b)** for sample 2; **(c)** Comparison between the swelling/shrinking behaviors of the two samples.

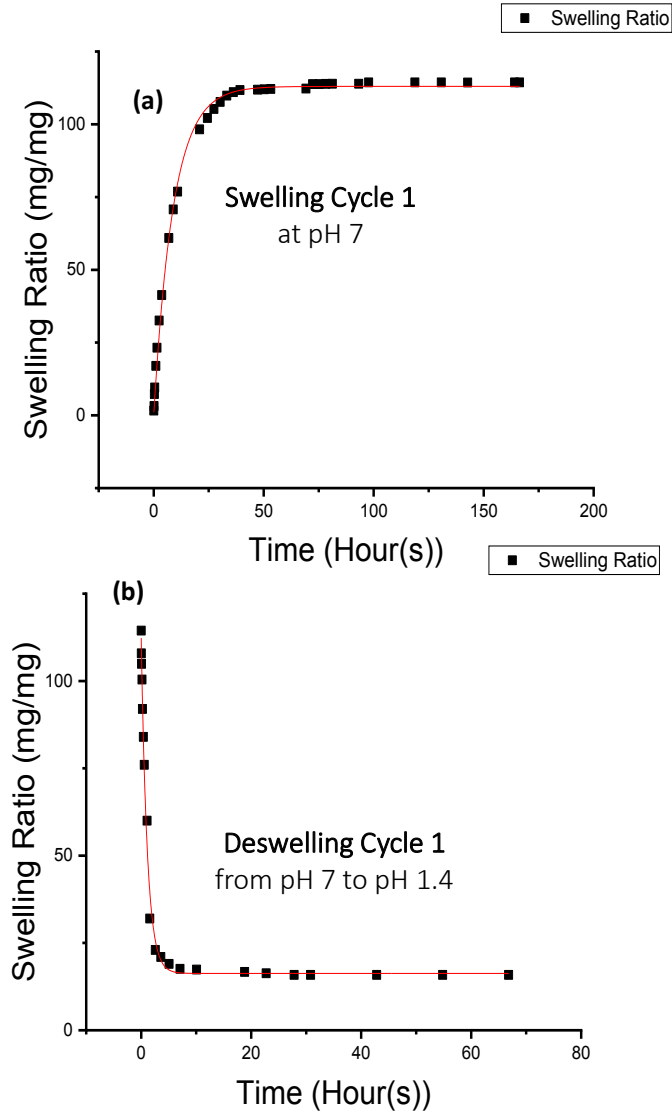


Fig. 4.10. Sample 1 cycle 1: **(a)** Swelling data when pH of the solution is 7; **(b)** Deswelling data for the when pH of the solution changes from 7 to 1.4.

In the Fig. 4.10 (a), the swelling rate and equilibrium swelling were calculated from the swelling ratio vs time plot as shown in figure 4.10 using the equation [56]:

$$S_t = S_e(1 - e^{-t/\tau}) \quad (1)$$

Where S_t is the swelling at time t , S_e is equilibrium swelling, t is the time any instantaneous time, τ is the rate parameter.

The swelling rate was estimated using the equation [56]:

$$SR = S_c/\tau \quad (2)$$

Where S_t is the swelling at time .

In Fig. 4.10 (b) when the hydrogel is dipped in pH 1.4 solution after removing it from the pH 7 solution, the deswelling rate and equilibrium swelling were obtained from the equation [56]:

$$S_{tD} = S_0 + (S_e - S_0)e^{-t/\tau} \quad (3)$$

Where S_{tD} , S_0 and S_e are the deswelling ratio at time t; equilibrium swelling ratios at pH 1.4 (the lower pH value) and at pH 7 (the highr pH value), respectively.

The deswelling rate was estimated using the equation [56]:

$$DSR = (S_e - S_{tD})/S_{tD} \quad (4)$$

Where S_{tD} is the deswelling at time τ_D .

In Fig. 4.11 (a) when the hydrogel makes a transition from pH 1.4 to pH 7, the swelling rate and equilibrium swelling were obtained from the equation [56]:

$$S_t = S_e - (S_e - S_0)e^{-t/\tau} \quad (5)$$

$$SR = (S_c - S_0)/\tau \quad (6)$$

In Fig. 4.11 (b) when the hydrogel is again dipped in pH 1.4 solution after removing from pH 7 solution, equations 3 and 4 are used to determine the deswelling equilibrium and deswelling rates.

In Fig. 4.12 (a) when the hydrogel is again immersed in pH 7 solution after taking it out from the pH 1.4 solution, equations 5 and 6 are used to determine the swelling equilibrium and swelling rates.

Fig. 4.12 (b) shows the deswelling of sample 1 when pH value was changed from 7 to 1.4. The deswelling equilibrium and deswelling rates were again calculated using equations 3 and 4.

Figures 4.13, 4.14 and 4.15 showed the swelling and deswelling behaviors for sample 2's three consecutive cycles. The swelling and deswelling curves were fitted using the above equations in the similar way as done for the sample 1.

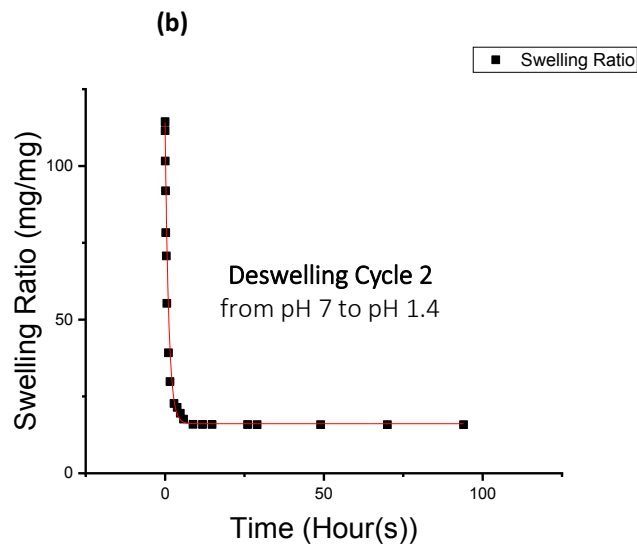
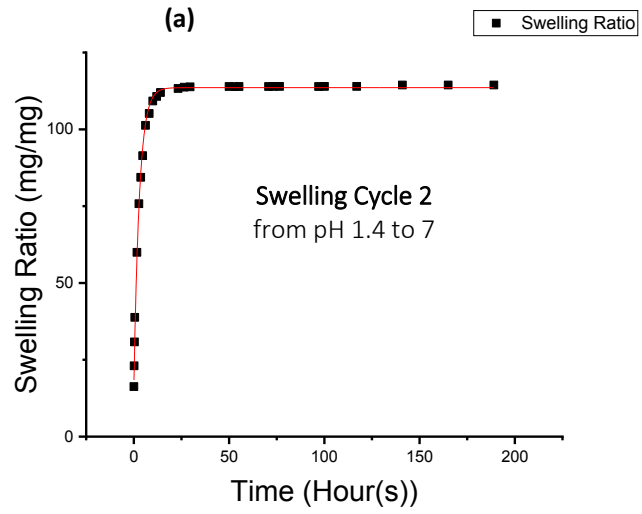


Fig. 4.11. Sample 1, cycle 2: **(a)** Swelling data when pH of the solution switches from 1.4 to 7; **(b)** Deswelling data when pH of the solution changes from 7 to 1.4.

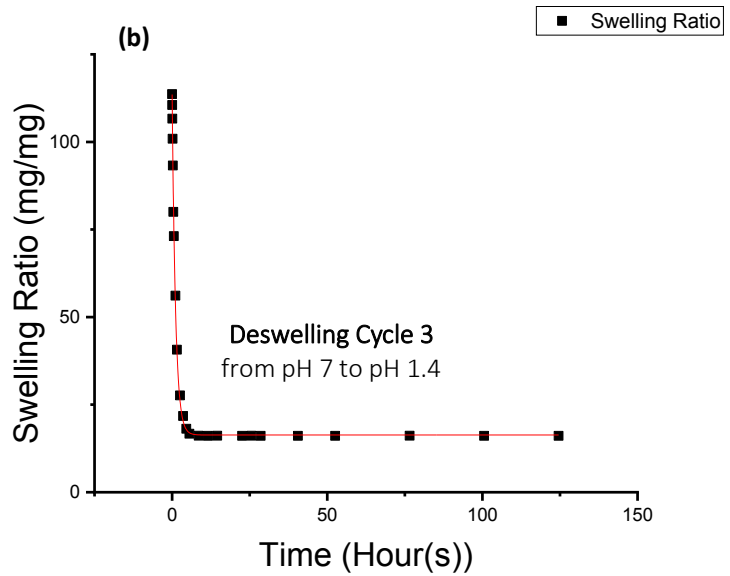
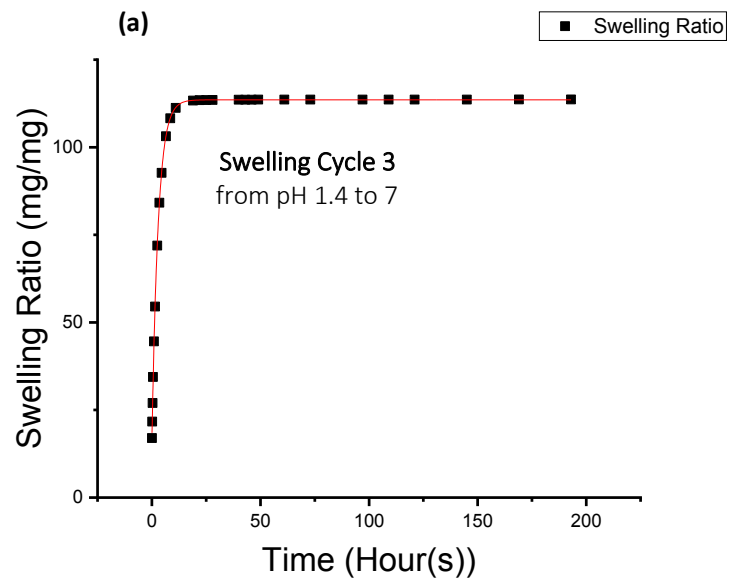


Fig. 4.12. Sample 1, cycle 3: **(a)** Swelling data when pH of the solution changes from 1.4 to 7; **(b)** Deswelling data when pH of the solution changes from 7 to 1.4.

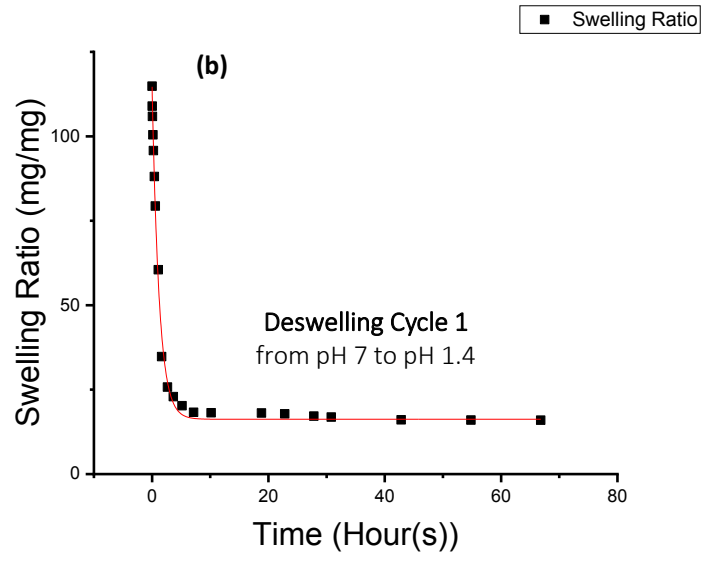
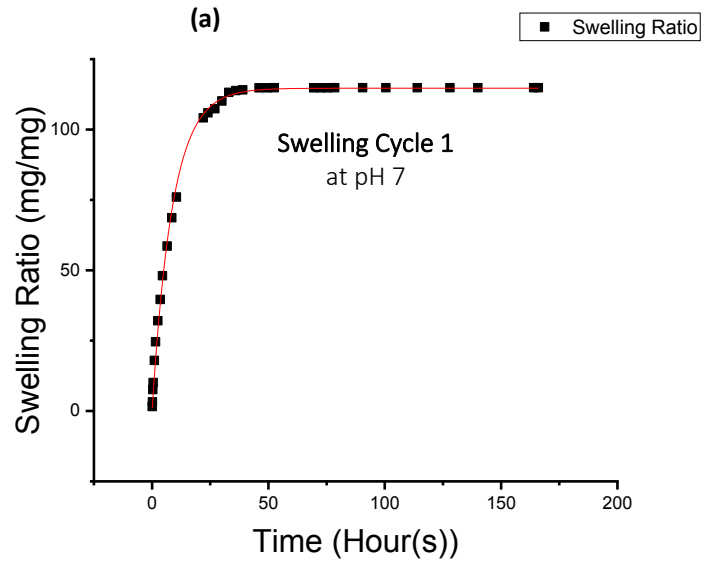


Fig. 4.13. Sample 2, cycle 1: **(a)** Swelling data when pH of the solution is 7; **(b)** Deswelling data when pH of the solution changes from 7 to 1.4.

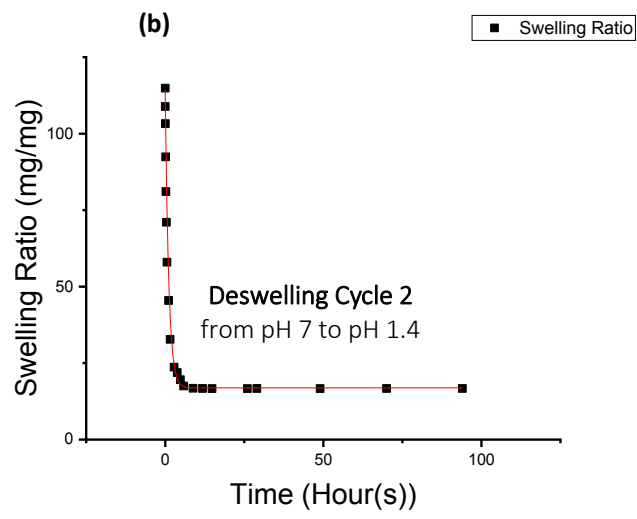
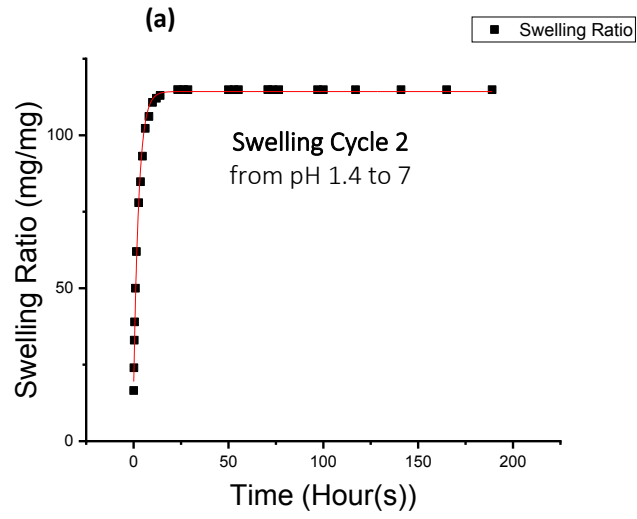


Fig. 4.14 Sample 2, cycle 2: **(a)** Swelling data when pH of the solution changes from 1.4 to 7; **(b)** Deswelling data when pH of the solution changes from 7 to 1.4.

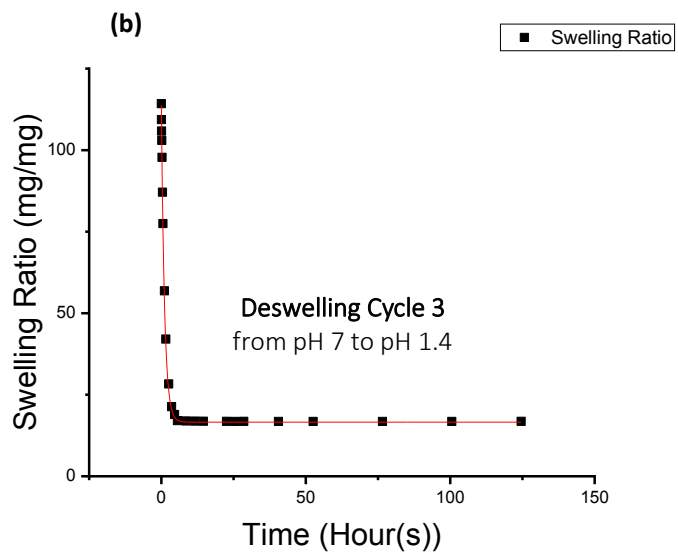
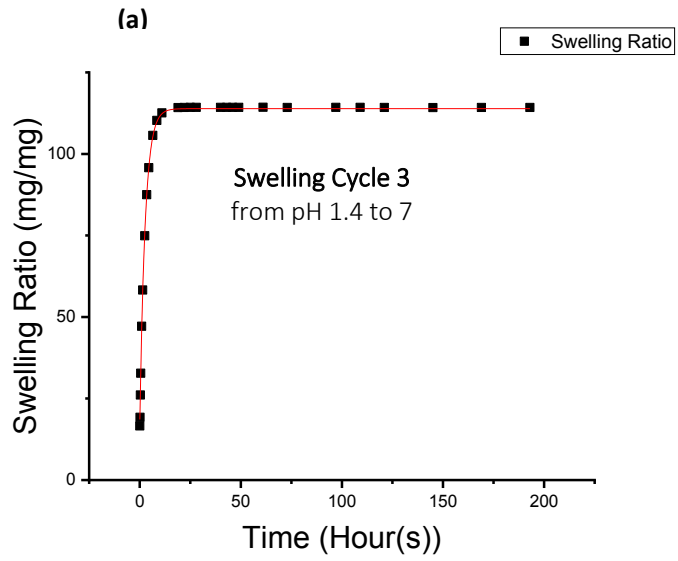


Fig. 4.15. Sample 2, cycle 3: (a) Swelling data when pH of the solution changes from 1.4 to 7; (b) Deswelling data when pH of the solution changes from 7 to 1.4

Table 4.1. Swelling and deswelling characteristics of the PAAVSA hydrogel Sample 1 because of pH reversibility between pH 7 and 1.4

Sample 1	Swelling		Deswelling (pH 7-1.4)	
Cycles	Swelling Equilibrium, S_e (mg/mg)	Swelling Rate, SR (mg/(mg.min))	Deswelling Equilibrium, S_0 (mg/mg)	Deswelling Rate, DSR (mg/(mg.min))
1	113.019 (pH 7)	0.134	16.270	0.913
2	113.569 (pH 1.4-7)	0.355	16.140	0.924
3	113.540 (pH 1.4-7)	0.359	16.340	0.932

Table 4.2. Swelling and deswelling characteristics of the PAAVSA hydrogel sample 2 because of pH reversibility between pH 7 and 1.4

Sample 2	Swelling		Deswelling (pH 7-1.4)	
Cycles	Swelling Equilibrium, S_e (mg/mg)	Swelling Rate, SR (mg/(mg.min))	Deswelling Equilibrium, S_0 (mg/mg)	Deswelling Rate, DSR (mg/(mg.min))
1	114.679 (pH 7)	0.138	16.230	0.859
2	114.290 (pH 1.4-7)	0.378	16.900	0.920
3	113.890 (pH 1.4-7)	0.390	16.590	0.919

The swelling/deswelling reversibility study for PAAVSA hydrogel weighing 84 mg stated in Tables 4.1 and 4.2 revealed excellent pH sensitivity and reversibility. It was found that in the second and third cycles, the swelling rate of the hydrogel increased nearly threefold while

the deswelling rate was still around 2.5 times faster. The comparatively higher deswelling rate is useful in pH-based chemical sensors, especially in the diagnosis of the diseases where pH of the diseased site swiftly goes very low.

Table 4.3. Values of swelling rate (SR) and equilibrium swelling (S_e) for the PAAVSA hydrogel samples [54].

Sample Weights (mg)	Swelling (pH 7)	
	Swelling Rate (SR) (mg/mg.min)	Swelling Equilibrium (S_e) (mg/mg)
84.07	0.134	113.019
84.29	0.138	114.679
101	0.153	148.41

The swelling/deswelling reversibility study for PAAVSA hydrogel samples weighing 84 mg was compared with the swelling measurement of PAAVSA hydrogel sample weighing 101 mg [54], and it was found that when the hydrogel is immersed in pH 7 solution, the swelling rates (SR) and swelling equilibriums (S_e) were relatively higher for the heavier sample.

4.3. Discussion

Tables 4.1 and 4.2 summarize the results found in our study and table 4.3 compares it with the finding in the earlier study made on the same PAAVSA hydrogel. The experimental findings show distinctly higher pH sensitivity for the PAAVSA hydrogel between pH values 1.4 and 7 confirming the results seen in the earlier works [1,2]. Samples having the same amount giving similar results validate its reproducibility also.

The swelling/deswelling study was taken in three cycles where the pH of the solution was alternatively changed from 7 to 1.4, and the results found in cycles 2 and 3 were almost similar, verifying its recyclability and making it a durable material that can withstand in large pH variation for long. The swelling/shrinking behavior is linked to the loading of drug molecules into the hydrogel matrix and the regulated release of drug molecules from the matrix [3]. It is seen in our study that the deswelling rate when the pH of the solution is changed from 7 to 1.4, is 0.9 mg/mg.min or 54 mg/mg.hr, which is very high and useful in disease diagnosis and remediation. The higher the rate of swelling/deswelling, the more effective and time-saving a sensing device will be [4]. Diseases like brain tumor where pH is around 5, dermatitis where pH of skin tissues is 6.6, ichthyosis (pH 4.6 and 5.3), and fungal infections (pH 5.1-5.7) have their pH less than skin tissue pH [6-8]. In these conditions, the PAAVSA hydrogel is highly applicable to get a faster and low-cost diagnosis. As soon as the pH of the site changes, the hydrogel will also show a similar swelling/shrinking behavior, which, in a sensing device (consisting of the hydrogel) can be reflected in other ways like change in voltage, capacitance, inductance, impedance, or resonance frequency etc. Moreover, when injected with drugs and also embedded with magnetic nanoparticles, the hydrogel can be upgraded to provide healing as well. For example, it can be used in magnetically targeted drug delivery to a diseased body site. The biocompatibility of PAAVSA has already been confirmed by evaluating it with HEK-293 cells, making it a much safer disease diagnosis and remedial alternative as compared to the other conventional counterparts [54]. For example, in GERD

disease, where the pH of the esophagus goes below 4 lesser than the pH in the normal state (pH 7), the PAAVSA hydrogel, with its swelling/shrinking response behavior in between the two pH values, can become a safer, faster and cost-effective tool in diagnosing the disease [2].

Chapter 5

Conclusions and Scope for Future

In summary, the work presented aimed at developing a sensing scheme for in vivo detection of any changes in chemical stimuli such as pH. To achieve this, we coupled a pH-sensitive hydrogel with a magnetic strip, and as there was any variation in the pH surrounding the hydrogel, it responded by swelling/shrinking or in another way, by vertically moving upward/downward. This change was detected by an Arduino sensor placed above the (hydrogel + magnetic strip) setup.

The hydrogels, as described in Chapter 2, have a unique advantage in passive sensors and actuators because of their smart property, which allows the chemical response to the surrounding environment's pH or glucose to be translated into reversible mechanical behavior (swelling and shrinking) without the use of an external power source. Hydrogels are also advantageous in the way that they can be chemically or biologically functionalized in crosslinking with molecules or other nanoscale entities such as superparamagnetic iron oxide nanoparticles (SPIONs). The hydrogels are potential candidates for making passive sensing devices owing to their custom functionalization properties. The pH or other analyte activated swelling/shrinking of a hydrogel can be applied to measure the analyte concentration indirectly by coupling it with a capacitive-inductive circuit, where only the capacitance varies, and other components remain constant so that a one-to-one relation between the analyte concentration and capacitance or resonant frequency can be obtained. Hydrogels, embedded with magnetic nanoparticles are also extremely effective in chemical sensing as well as in targeted and controlled drug delivery systems. In magnetic nanoparticles embedded hydrogels, the magnetic permeability is modulated when there is a change in hydrogel volume due to a change in analyte concentration. This modulation can be monitored by integrating the ferrogel in an LCR

circuit and a readout coil in a properly aligned proximity and seeing the resonant frequency change due to analyte concentration variation. Additional electrical components, such as capacitance and resistance, influence resonant frequency changes. The ferrogel sensor output must be a function of a single variable, in this case the inductance, in order to be useful. As a result, the future direction must involve the investigation of a way for reducing the undesirable responsiveness to capacitance and resistance by incorporating a reference element in near proximity (only affecting resistance and capacitance).

The future direction in the fabrication of bio/chemical sensors must take care of making hydrogel-based, low cost, simple to fabricate, precise, fast responsive and commercially viable in order to make them scalable and practical utility.

References

- [1] Aoi, Wataru, and Yoshinori Marunaka. "Importance of pH homeostasis in metabolic health and diseases: crucial role of membrane proton transport." *BioMed research international* 2014 (2014).
- [2] Clarrett, Danisa M., and Christine Hachem. "Gastroesophageal reflux disease (GERD)." *Missouri medicine* 115.3 (2018): 214.
- [3] Hunt, Richard H. "Importance of pH control in the management of GERD." *Archives of internal medicine* 159.7 (1999): 649-657.
- [4] Liu, Shuang, et al. "Research on gastroesophageal reflux disease based on dynamic features of ambulatory 24-hour esophageal pH monitoring." *Computational and mathematical methods in medicine* 2017 (2017).
- [5] Swietach, Pawel, et al. "The chemistry, physiology and pathology of pH in cancer." *Philosophical Transactions of the Royal Society B: Biological Sciences* 369.1638 (2014): 20130099.
- [6] Zhang, Xiaomeng, Yuxiang Lin, and Robert J. Gillies. "Tumor pH and its measurement." *Journal of Nuclear Medicine* 51.8 (2010): 1167-1170.
- [7] Danby, Simon G., and Michael J. Cork. "pH in atopic dermatitis." *pH of the Skin: Issues and Challenges* 54 (2018): 95-107.
- [8] Cornet, Muriel, and Claude Gaillardin. "pH signaling in human fungal pathogens: a new target for antifungal strategies." *Eukaryotic cell* 13.3 (2014): 342-352.
- [9] Vylkova, Slavena. "Environmental pH modulation by pathogenic fungi as a strategy to conquer the host." *PLoS pathogens* 13.2 (2017): e1006149.
- [10] Mobasser, Majid, et al. "Prevalence and incidence of type 1 diabetes in the world: a systematic review and meta-analysis." *Health promotion perspectives* 10.2 (2020): 98.
- [11] Khan, Moien Abdul Basith, et al. "Epidemiology of type 2 diabetes—global burden of disease and forecasted trends." *Journal of epidemiology and global health* 10.1 (2020): 107.
- [12] Tripathy, Jaya Prasad, et al. "Prevalence and risk factors of diabetes in a large community-based study in North India: results from a STEPS survey in Punjab, India." *Diabetology & metabolic syndrome* 9.1 (2017): 1-8.

- [13] Al-Mawali, Adhra, et al. "Prevalence and risk factors of diabetes in a large community-based study in the Sultanate of Oman: STEPS survey 2017." *BMC Endocrine Disorders* 21.1 (2021): 1-11.
- [14] Animaw, Worku, and Yeshaneh Seyoum. "Increasing prevalence of diabetes mellitus in a developing country and its related factors." *PloS one* 12.11 (2017): e0187670.
- [15] Wild, Sarah, et al. "Global prevalence of diabetes: estimates for the year 2000 and projections for 2030." *Diabetes care* 27.5 (2004): 1047-1053.
- [16] Zhang, Ping, et al. "Global healthcare expenditure on diabetes for 2010 and 2030." *Diabetes research and clinical practice* 87.3 (2010): 293-301.
- [17] Bansode, Balasaheb, and Suresh Jungari. "Economic burden of diabetic patients in India: a review." *Diabetes & Metabolic Syndrome: Clinical Research & Reviews* 13.4 (2019): 2469-2472.
- [18] Yoon, Ji-Won, and Hee-Sook Jun. "Autoimmune destruction of pancreatic β cells." *American journal of therapeutics* 12.6 (2005): 580-591. [19]
- [19] Klonoff, David C. "Continuous glucose monitoring: roadmap for 21st century diabetes therapy." *Diabetes care* 28.5 (2005): 1231-1239.
- [20] Klonoff, David C. "Noninvasive blood glucose monitoring." *Diabetes care* 20.3 (1997): 433-437.
- [21] Gough, D. A., J. C. Armour, and D. A. Baker. "Advances and prospects in glucose assay technology." *Diabetologia* 40.2 (1997): S102-S107.
- [22] Koschwanez, Heidi E., and William M. Reichert. "In vitro, in vivo and post explantation testing of glucose-detecting biosensors: current methods and recommendations." *Biomaterials* 28.25 (2007): 3687-3703.
- [23] Pickup, John C., Gill W. Shaw, and Denzil J. Claremont. "Potentially-implantable, amperometric glucose sensors with mediated electron transfer: improving the operating stability." *Biosensors* 4.2 (1989): 109-119.
- [24] Bindra, Dilbir S., et al. "Design and in vitro studies of a needle-type glucose sensor for subcutaneous monitoring." *Analytical chemistry* 63.17 (1991): 1692-1696.
- [25] Armour, Jon C., et al. "Application of chronic intravascular blood glucose sensor in dogs." *Diabetes* 39.12 (1990): 1519-1526.

- [26] Shichiri, Motoaki, et al. "Enhanced, simplified glucose sensors: long-term clinical application of wearable artificial endocrine pancreas." *Artificial organs* 22.1 (1998): 32-42.
- [27] Tse, Pius HS, and David A. Gough. "Time-dependent inactivation of immobilized glucose oxidase and catalase." *Biotechnology and bioengineering* 29.6 (1987): 705-713.
- [28] Gough, David A., et al. "Function of an implanted tissue glucose sensor for more than 1 year in animals." *Science Translational Medicine* 2.42 (2010): 42ra53-42ra53.
- [29] Coté, Gerald L., Martin D. Fox, and Robert B. Northrop. "Noninvasive optical polarimetric glucose sensing using a true phase measurement technique." *IEEE Transactions on biomedical engineering* 39.7 (1992): 752-756.
- [30] Burmeister, Jason J., and Mark A. Arnold. "Evaluation of measurement sites for noninvasive blood glucose sensing with near-infrared transmission spectroscopy." (1999): 1621-1627.
- [31] Stuart, Douglas A., et al. "Glucose sensing using near-infrared surface-enhanced Raman spectroscopy: gold surfaces, 10-day stability, and improved accuracy." *Analytical chemistry* 77.13 (2005): 4013-4019.
- [32] Tierney, Sven, Dag Roar Hjelme, and Bjørn Torger Stokke. "Determination of swelling of responsive gels with nanometer resolution. Fiber-optic based platform for hydrogels as signal transducers." *Analytical chemistry* 80.13 (2008): 5086-5093.
- [33] Tierney, Sven, Sondre Volden, and Bjørn Torger Stokke. "Glucose sensors based on a responsive gel incorporated as a Fabry-Perot cavity on a fiber-optic readout platform." *Biosensors and Bioelectronics* 24.7 (2009): 2034-2039.
- [34] Clarrett, Danisa M, and Christine Hachem. "Gastroesophageal Reflux Disease (GERD)." *Missouri medicine* vol. 115,3 (2018): 214-218.
- [35] Forootan, Mojgan et al. "Advances in the Diagnosis of GERD Using the Esophageal pH Monitoring, Gastro-Esophageal Impedance-pH Monitoring, And Pitfalls." *Open access Macedonian journal of medical sciences* vol. 6,10 1934-1940. 24 Oct. 2018, doi:10.3889/oamjms.2018.410
- [36] Liu, Shuang, et al. "Research on gastroesophageal reflux disease based on dynamic features of ambulatory 24-hour esophageal pH monitoring." *Computational and mathematical methods in medicine* 2017 (2017).

- [37] Tutuian, Radu, and Donald O. Castell. "Gastroesophageal reflux monitoring: pH and impedance." *GI Motility online* (2006).
- [38] Holtz, John H., and Sanford A. Asher. "Polymerized colloidal crystal hydrogel films as intelligent chemical sensing materials." *Nature* 389.6653 (1997): 829-832.
- [39] Mujumdar, Siddhartha K., and Ronald A. Siegel. "Introduction of pH-sensitivity into mechanically strong nanoclay composite hydrogels based on N-isopropylacrylamide." *Journal of Polymer Science Part A: Polymer Chemistry* 46.19 (2008): 6630-6640.
- [40] Tanaka, Toyochi, and David J. Fillmore. "Kinetics of swelling of gels." *The Journal of Chemical Physics* 70.3 (1979): 1214-1218.
- [41] Siegel, Ronald A., et al. "Hard and soft micro-and nanofabrication: An integrated approach to hydrogel-based biosensing and drug delivery." *Journal of controlled release* 141.3 (2010): 303-313.
- [42] Gupta, Piyush, Kavita Vermani, and Sanjay Garg. "Hydrogels: from controlled release to pH-responsive drug delivery." *Drug discovery today* 7.10 (2002): 569-579.
- [43] Gulrez, Syed KH, Saphwan Al-Assaf, and Glyn O. Phillips. "Hydrogels: methods of preparation, characterisation and applications." *Progress in molecular and environmental bioengineering-from analysis and modeling to technology applications* 117150 (2011).
- [44] Ottenbrite, Raphael M., Samuel J. Huang, and Kinam Park. *Hydrogels and biodegradable polymers for bioapplications*. Vol. 627. No. 2. Washington, DC: American Chemical Society, 1996.
- [45] Zhao, Xuanhe, et al. "Active scaffolds for on-demand drug and cell delivery." *Proceedings of the National Academy of Sciences* 108.1 (2011): 67-72.
- [46] Bashir, R., et al. "Micromechanical cantilever as an ultrasensitive pH microsensor." *Applied Physics Letters* 81.16 (2002): 3091-3093.
- [47] Chatterjee, Sudipta, and Patrick Chi-leung Hui. "Stimuli-responsive hydrogels: An interdisciplinary overview." *Hydrogels—smart materials for biomedical applications* (2018): 1-23.
- [48] Shi, Qiang, et al. "Bioactuators based on stimulus-responsive hydrogels and their emerging biomedical applications." *NPG Asia Materials* 11.1 (2019): 1-21.
- [49] Babincova, Melania, and Peter Babinec. "Magnetic drug delivery and targeting: principles and applications." *Biomed Pap Med Fac Univ Palacky Olomouc Czech Repub* 153.4 (2009): 243-50.

- [50] Pankhurst, Quentin A., et al. "Applications of magnetic nanoparticles in biomedicine." *Journal of physics D: Applied physics* 36.13 (2003): R167.
- [51] Saini, S. A. N. J. A. Y., et al. "Magnetism: a primer and review." *American Journal of Roentgenology* 150.4 (1988): 735-743.
- [52] Butler, Robert F., and Robert F. Butler. *Paleomagnetism: magnetic domains to geologic terranes*. Vol. 319. Boston: Blackwell Scientific Publications, 1992.
- [53] Demas, Vasiliki, and Thomas J. Lowery. "Magnetic resonance for in vitro medical diagnostics: superparamagnetic nanoparticle-based magnetic relaxation switches." *New Journal of Physics* 13.2 (2011): 025005.
- [54] Singh, Rinki, et al. "An efficient pH sensitive hydrogel, with biocompatibility and high reusability for removal of methylene blue dye from aqueous solution." *Reactive and Functional Polymers* 144 (2019): 104346.
- [55] Wang, David, et al. "A study of the swelling and model protein release behaviours of radiation-formed poly (N-vinyl 2-pyrrolidone-co-acrylic acid) hydrogels." *Radiation Physics and Chemistry* 80.2 (2011): 207-212.
- [56] Hong, R. Y., T. T. Pan, and H. Z. Li. "Microwave synthesis of magnetic Fe₃O₄ nanoparticles used as a precursor of nanocomposites and ferrofluids." *Journal of Magnetism and Magnetic Materials* 303.1 (2006): 60-68.
- [57] Anirudhan, T. S., and S. R. Rejeena. "Poly (methacrylic acid-co-vinyl sulfonic acid)-grafted-magnetite/nanocellulose superabsorbent composite for the selective recovery and separation of immunoglobulin from aqueous solutions." *Separation and Purification Technology* 119 (2013): 82-93.
- [58] Anirudhan, T. S., A. R. Tharun, and S. R. Rejeena. "Investigation on poly (methacrylic acid)-grafted cellulose/bentonite superabsorbent composite: synthesis, characterization, and adsorption characteristics of bovine serum albumin." *Industrial & engineering chemistry research* 50.4 (2011): 1866-1874.
- [59] Park, J. H., A. Kim, and B. Ziaie. "Batch-fabricated hydrogel/polymeric-magnet bilayer for wireless chemical sensing." *2015 28th IEEE International Conference on Micro Electro Mechanical Systems (MEMS)*. IEEE, 2015.